scientific reports

OPEN

Non-targeted LC-MS metabolomics reveals serum metabolites for high-altitude adaptation in Tibetan donkeys

Jing Wang[1,8], Yulong Feng[3,8], Shibo Xu[1], Ngodrup Tenzin[4], Haiyu Han[5], Dehong Gong[6], Fengxin Liu[7], Yujiang Sun[1,2]✉ & Shuqin Liu[1,2]✉

Tibetan donkeys inhabit the harsh environment of the Qinghai-Tibet Plateau. Research on serum metabolites related to their high-altitude adaptation is limited compared to other livestock. We used liquid chromatography-mass spectrometry (LC-MS) to analyze serum samples from healthy adult donkeys in Shigatse, Changdu, and Dezhou to evaluate the effects of high altitudes on serum metabolites. Metabolomics analysis identified 443 differential metabolites (DMs) across the three groups, meeting criteria of VIP ≥ 1, *p-value < 0.05*, and Fold-Change ≥ 1.2 or ≤ 0.5. Significant upregulation was observed in deoxycholic acid, vitamin A, vitamin C, flavin mononucleotide, n-acetylserotonin, N'-formyl-kynurenine, calcidiol, and adenosine monophosphate in the high-altitude group compared to the low-altitude control group. The DMs were involved in processes such as bile secretion, vitamin digestion and absorption, tryptophan metabolism, and parathyroid hormone synthesis, secretion, and action. All these are crucial for nutrient metabolism, immune function, and antioxidant stress response. This study constructed a metabolomics dataset of Tibetan donkey serum and revealed differential metabolites among donkeys from different geographic regions and environments. The results offer crucial insights into the adaptive regulatory mechanisms.

The Qinghai-Tibet Plateau experiences severe cold, low oxygen levels, high ultraviolet radiation, and strong winds[1]. Animals have adapted to these harsh environmental factors through long-term natural selection, forming unique groups suited for high-altitude environments[2].

Tibetan donkeys in high-altitude regions showed a stronger tolerance to hypoxia and a higher metabolism of cellulose and hemicellulose. These changes contribute to their survival in harsh habitats[3]. Guo et al. found higher flora diversity and richness in Tibetan donkeys than in Dezhou donkeys at low altitudes[4]. A study on the high-altitude adaptation of Tibetan donkeys identified the role of the *EGLN1* gene in their adaptation[5]. Zhou et al. conducted second-generation sequencing on six donkey breeds to explore genetic variations related to high-altitude adaptation[6]. Luo et al. identified 16 novel amino acid variants in proteins encoded by Tibetan donkeys' mitochondrial DNA. These variants may affect mitochondrial energy production efficiency and enhance adaptation to cold and hypoxic conditions in the Qinghai-Tibet Plateau[7]. In summary, these studies have revealed adaptation mechanisms in donkeys in extreme environments, focusing mainly on the intestinal flora and genes of Tibetan donkeys. However, compared with other livestock, research on the high-altitude adaptability of Tibetan donkeys is scarce[8–10].

Metabolites are a key means of communication between the host and the producer microbes[11]. Metabolomics, through liquid chromatography-tandem mass spectrometry (LC-MS/MS), can achieve high-throughput, high-sensitivity, wide-coverage, and accurate metabolite detection and analysis[12,13]. It can reveal metabolic changes in organisms during disease development, drug action, environmental exposure, and other processes[14–17]. Such studies provide new insights and methods for disease diagnosis, treatment, and prevention.

[1]College of Animal Science and Technology, Qingdao Agricultural University, Qingdao, Shandong, China. [2]Shandong Equine Genetic Resource Gene Bank, Qingdao, Shandong, China. [3]College of Animal Science and Technology, Shihezi University, Shihezi, Xinjiang, China. [4]Tibet Autonomous Region Animal Husbandry Station, Tibet, China. [5]Changdu Animal Husbandry General Station, Changdu, Tibet, China. [6]Qingdao Agricultural University, Qingdao, Shandong, China. [7]Shandong Dezhou School, Dezhou, Shandong, China. [8]Jing Wang and Yulong Feng have contributed equally to this work. ✉email: s36s@163.com; sqliu12@qau.edu.cn
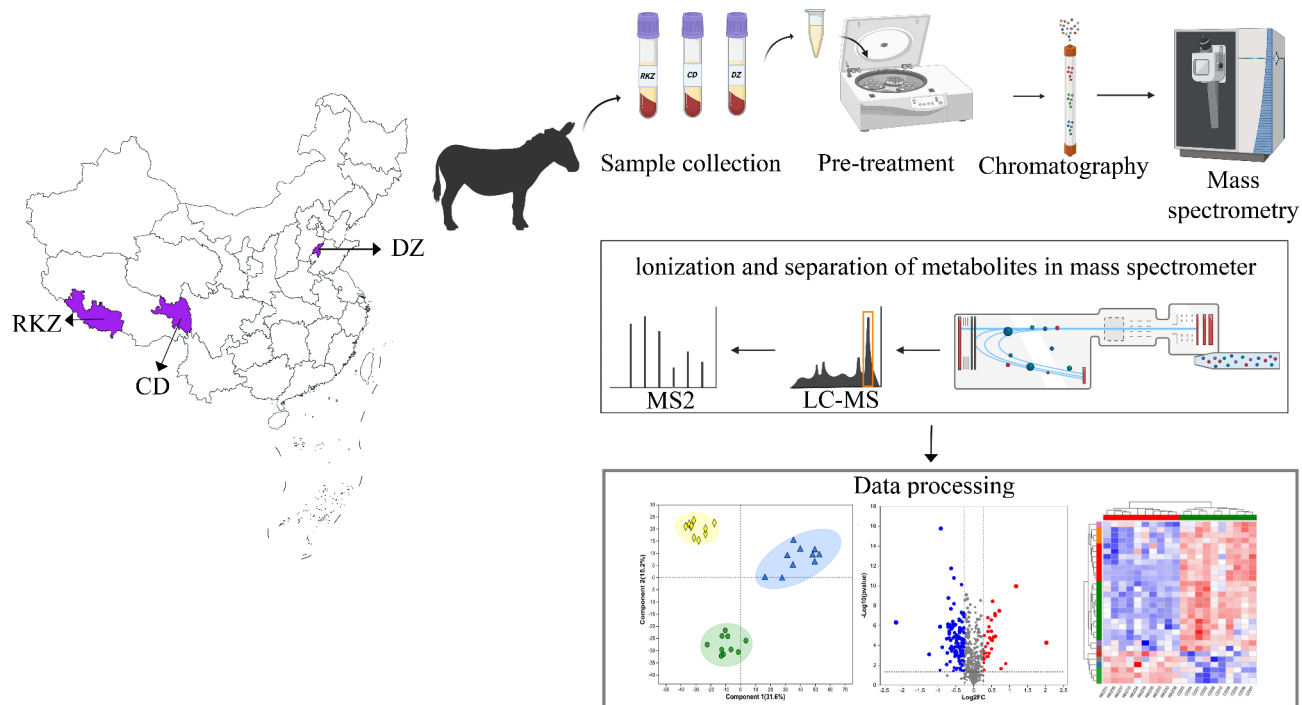
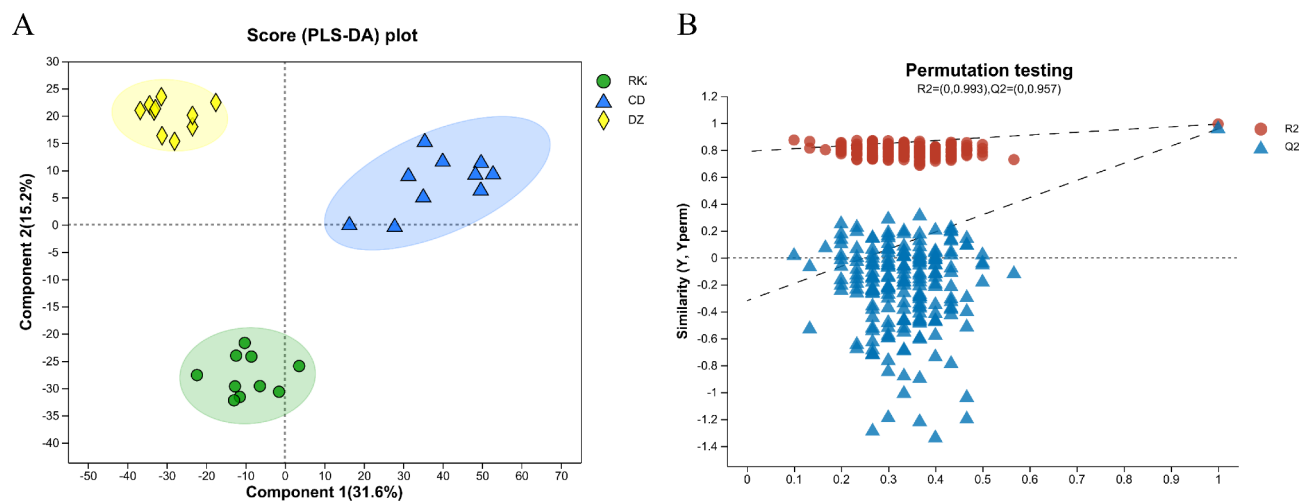**Fig. 1**. Workflow overview of the comprehensive analysis of metabolome in Tibetan and Dezhou donkeys.

Fig. 2. PLS-DA model score (**A**) and model validation (**B**) for the three groups of serum metabolome samples under the combined ion mode. The abscissa represents the permutation reservation of the permutation test. The ordinate represents the values of the substitution tests for R2 (the red dot) and Q2 (the blue triangle). The two dotted lines represent the R2 and Q2 regression lines.

This study explored the specific mechanism of high-altitude adaptation in Tibetan donkeys using serum non-targeted metabolomics analyses comparing high-altitude Tibetan donkeys and low-altitude Dezhou donkeys (Fig. 1). Our results highlight the adaptive metabolism of donkeys at high altitudes and elucidate its potential mechanism, and these screened biomarkers may provide new targets for donkey breeding.

Results

Partial least squares discrimination analysis (PLS-DA)

A total of 678 metabolites were detected, including 342 and 336 metabolites in the positive (ESI+) and negative ion modes (ESI−), respectively. PLS-DA results showed that Component 1 was 31.6%, and Component 2 was 15.2%. The RKZ, CD, and DZ groups were effectively divided into three categories in the combined ion mode, indicating significant differences in their metabolite phenotypes (Fig. 2A). The validation of the PLS-DA
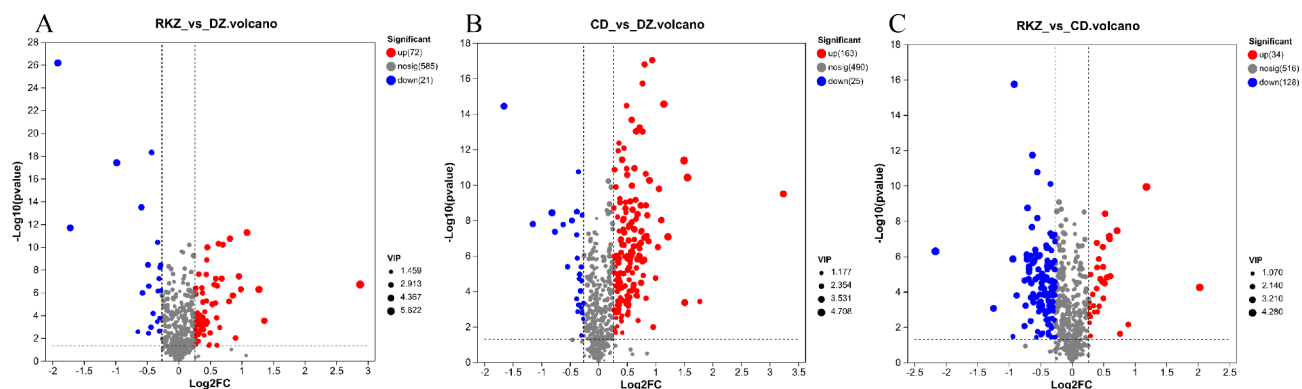
Fig. 3. Volcano maps of DMs in the combined ion model. Red, blue, and gray represent upregulation, downregulation, and no change, respectively.
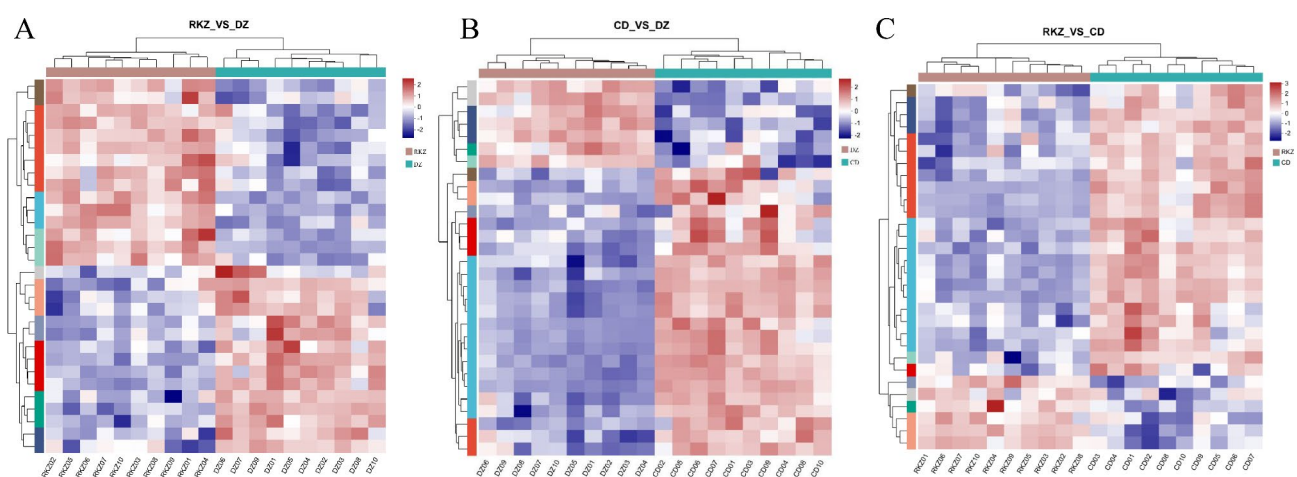

Fig. 4. Heatmaps of the top 30 DMs ranked by VIP values in serum with a cutoff value of VIP > 1 and $p < 0.05$ (t-tests). Each row represents a metabolite and the column corresponds to a sample. The color intensity indicates the relative abundance of respective metabolites, with warmer colors reflecting higher levels and cooler colors indicating lower levels. The hierarchical clustering of both metabolites and samples highlights patterns and relationships among the DMs.

model showed that in the combined ion mode, the R2 and Q2 intercepts of the model reached 0.993 and 0.957, respectively. This indicated that the model fitted well, and was highly predictable and suitable for subsequent data analysis (Fig. 2B). The Model Overview and Model parameters are shown in Supplementary Document 1.

Identification of DMs
According to VIP ≥ 1, $p < 0.05$, and Fold-Change ≥ 1.2[18] or ≤ 0.5, 93 DMs were identified in the RKZ_VS_DZ group, including 72 up-regulated and 21 down-regulated (Fig. 3A). In the CD_VS_DZ group, 188 DMs were identified (83 in ESI + and 105 in ESI−), with 163 up-regulated and 25 down-regulated (Fig. 3B). In the RKZ_VS_CD group, 162 DMs were identified (65 in ESI + and 97 in ESI−), including 34 up-regulated and 128 down-regulated (Fig. 3C).

Furthermore, the top 30 DMs in each of the three groups were selected for cluster analysis. Each of the three difference groups was clustered into two categories, indicating their similar functional annotations or belonging to the same metabolic pathway (Fig. 4). The expression differences between different samples were obvious.

KEGG enrichment analysis of DMs
KEGG pathway results showed that DMs mainly clustered in bile secretion, parathyroid hormone synthesis, secretion and action, vitamin digestion and absorption, mTOR signaling pathway, and PI3K-Akt signaling pathway in the RKZ_VS_DZ group (Fig. 5A, Table 1). Metabolites in the CD_VS_DZ group mainly concentrated in vitamin digestion and absorption, tryptophan metabolism, fluid shear stress and atherosclerosis, bile secretion, and HIF-1 signaling pathway metabolism (Fig. 5B, Table 1). Metabolites in the RKZ_VS_CD group mainly concentrated in tryptophan metabolism, vitamin digestion and absorption, parathyroid hormone synthesis, secretion and action, bile secretion, and steroid hormone biosynthesis (Fig. 5C, Table 1).
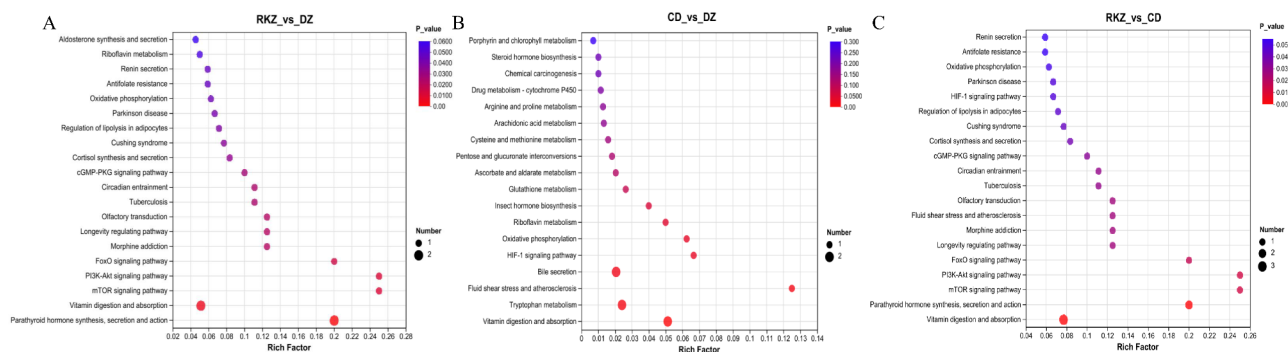
Fig. 5. Classification and KEGG pathway analysis of DMs. The A), B), and C) bubble plots depict DMs mapped to their respective metabolic pathways. The dotted lines indicate the significance cutoff with a p-value of 0.05. The size of the bubble corresponds to the number of DMs in the respective KEGG pathway[19].

Group	Pathway description	P_value	Metabolites	RT	Regulate	M/Z
RKZ_VS_DZ	Bile secretion	0.0054	Deoxycholic Acid	6.6747	Up	391.2849
	Vitamin digestion and absorption	0.0106	Vitamin A,	6.9643	Up	331.2273
			Flavin Mononucleotide	6.4958	Up	391.2849
	Parathyroid hormone synthesis, secretion, and action	0.0058	Calcidiol,	7.2717	Up	421.3108
			Adenosine monophosphate	0.9318	Up	346.0552
	mTOR signaling pathway	0.0008	Adenosine monophosphate	0.9318	Up	346.0552
	PI3K-Akt signaling pathway	0.0465	Adenosine monophosphate	0.9318	Up	346.0552
CD_VS_DZ	Fluid shear stress and atherosclerosis	0.0194	Hyaluronic acid	4.8211	Up	439.1595
	Bile secretion	0.0226	Deoxycholic Acid	6.4614	Up	341.1236
	Tryptophan metabolism	0.0169	N'-Formylkynurenine	3.4485	Up	235.0718
	Vitamin digestion and absorption	0.0039	Vitamin C,	0.9318	Up	351.0563
			Flavin Mononucleotide	6.4958	Up	477.0797
	HIF-1 signaling pathway	0.0360	Vitamin C	0.9318	Up	351.0563
RKZ_VS_CD	Tryptophan metabolism	0.0001	N-Acetylserotonin,	4.4431	Up	219.1127
			Melatonin,	2.9173	Up	277.1189
			N'-Formylkynurenine	3.4485	Down	235.0718
	Steroid hormone biosynthesis	0.0033	Estradiol-17beta 3-sulfate,	6.3856	Down	351.1266
			Calcidiol,	7.2717	Up	421.3108
			Estrone 3-sulfate	6.358	Down	349.1110
	Bile secretion	0.0031	Deoxycholic Acid	6.3856	Up	6.3856
	Parathyroid hormone synthesis, secretion, and action	0.0004	Calcidiol,	7.2717	Up	421.3108
			Adenosine monophosphate	0.9318	Up	346.0552
	Vitamin digestion and absorption	0.0002	Flavin Mononucleotide,	6.4958	Down	477.0797
			Vitamin A,	6.9643	Up	331.2273
			Vitamin C	0.9318	Down	351.0563

Table 1. KEGG enrichment statistics.

Discussion

High-altitude adaptation involves not only genetic regulation but also complex physiological and biochemical responses. We used an untargeted LC-MS metabolomics method to analyze serum metabolism to understand high-altitude adaptation in Tibetan donkeys.

In the three test groups (RKZ, CD, and DZ), we found that the metabolite DCA (deoxycholic acid) was significantly enriched in bile secretion metabolic pathways. Cholic acid (BAs), produced through bile secretion, plays a crucial role as a biological regulator regulating glucose, fat, and energy metabolism[20]. As a principal constituent of bile, DCA has immunomodulatory and anti-inflammatory properties[21,22]. It facilitates fat digestion and absorption in the small intestine and also contributes to cholesterol (CHOL) metabolism and induces gallbladder contraction to regulate gallbladder function[23]. CHOL, a primary component of cell membranes, is crucial for membrane formation, maintenance, and signal transduction[24]. We found significant enrichment of DCA in the bile secretion pathway across various groups, implying that Tibetan donkeys may

have enhanced lipid digestion and absorption due to modulated bile secretion. This potentially improves their energy metabolism and adaptability to high-altitude environments.

Similarly, the DMs of vitamin A, vitamin C, and FMN were primarily enriched in the vitamin digestion and absorption pathways in the three distinct elevation groups. Vitamin A has antioxidant properties that enable direct removal of reactive oxygen species, enhance antioxidant oxidase activity, and promote antioxidant defense mechanisms[25]. FMN, the active form of vitamin B2, is vital for energy metabolism and participates in various biochemical reactions[26–28]. Similarly, vitamin C inhibits hypoxia-induced mitochondrial damage and apoptosis in human endothelial cells[29]. Vitamin C potentially contributes to the maintenance of the central vascular system in the Tibetan donkey's plateau environment. Additionally, studies have shown that vitamin C can promote vasodilation and regulate peripheral vascular responses to local cold stimulation in high-altitude populations[30]. Thus, vitamins A and C may support the adaptability of Tibetan donkeys in the plateau environment through their antioxidant and vascular regulation effects. Vitamin metabolism might enhance their immunity and production performance.

In the CD_VS_DZ and RKZ_VS_CD groups, DMs such as NFK, n-acetylserotonin, and melatonin were enriched in tryptophan metabolism. Tryptophan metabolism is closely linked to carbohydrate, protein, and fat metabolism, as well as oxidative stress and inflammation regulation[31,32]. Moreover, tryptophan regulates immunity, neuronal function, and intestinal homeostasis through kynurenine metabolism[33]. Previous research has shown that Tibetan donkeys have significantly higher heme levels than plain donkeys under hypoxic conditions, with heme dioxygenase content increasing with heme levels at high altitudes. Heme dioxygenase catalyzes L-tryptophan conversion to N-formyl kynurenine (NFK), initiating tryptophan catabolism[34]. At high altitudes, light, temperature, and oxygen levels influence animal circadian rhythms. Particularly, melatonin plays a crucial role in the regulation and promotion of sleep. Melatonin is synthesized in the pineal gland from tryptophan conversion to serotonin[35]. It plays essential roles in circadian rhythm regulation, sleep cycles, and immune function[36]. Typically, less than 5% of tryptophan is utilized for serotonin and melatonin synthesis, and the remaining 95% is metabolized via the kynurenine pathway in the liver[37,38]. High-altitude living can elevate pro-inflammatory cytokines and glucocorticoids, enhancing tryptophan metabolism through the kynurenine pathway[39,40]. Consequently, animals at high altitudes may have increased energy production due to upregulated tryptophan biosynthesis in response to hypoxic stress[35]. This suggests that robust tryptophan metabolism in high-altitude donkeys potentially aids basal metabolism in such environments, enhancing hypoxia endurance.

In CD_VS_DZ and RKZ_VS_CD groups, calcidiol and AMP DMs were both enriched in parathyroid hormone (PTH) synthesis and secretion pathways. PTH synthesis and secretion are primarily regulated by serum calcium levels, with additional influence from factors such as vitamin D and neurotransmitters[41]. PTH regulates calcium levels[42], and calcidiol is a hydroxylated form of vitamin D3[43–46]. During hypoxia, diminished cellular adenosine triphosphate (ATP) levels activate adenosine monophosphate-activated protein kinase (AMPK), which indirectly fosters autophagy via nodular sclerosis complex 2 phosphorylation[47]. AMPK activity responds to intracellular energy status, particularly changes in the ATP/AMP ratio. Reduced ATP and elevated AMP levels, which indicate increased cellular energy expenditure, augment AMPK activity, modulate cellular energy metabolism, and maintain energy balance[48,49]. AMPK activation is influenced by energy status and pathological conditions such as glucose deficiency, ischemia, hypoxia, and oxidative stress[50]. Overall, AMP plays an important role in Tibetan donkeys' adaptation to high altitudes.

Materials and methods
Sample collection
A total of 30 blood samples, 10 from each region, were collected from donkeys in three regions: Shigatse (RKZ, 5,000 m above sea level) and Changdu (CD, 3,500 m above sea level) in Tibet, as well as Dezhou (DZ, 38 m above sea level) in Shandong. All subjects were adult healthy donkeys aged 5–10 years, in medium condition, and fed with local feed. Blood samples were collected using disposable vacuum coagulant tubes and left at room temperature for 20 min. They were then centrifuged at 12,000 rpm for 10 min to separate the serum. The serum samples were promptly frozen in liquid nitrogen for subsequent non-targeted metabolomics detection. This study was approved by the Institutional Animal Care and Use Committee (IACUC) of Qingdao Agricultural University.

Sample preparation
The serum samples were analyzed using the LC-MS (Thermo Scientific, Vanquish Horizon UHPLC System-Q Exactive HF-X) platform. After thawing at room temperature, 100 μL of each sample was transferred into 1.5 mL centrifuge tubes, and 300 μL of methanol was added. An internal standard solution of 2-chloro-l-phenylalanine (0.02 mg/mL), prepared by mixing equal volumes of methanol and acetonitrile, was added. The solution was vortex-mixed for 30 s and subjected to low-temperature ultrasound extraction for 30 min at 5 °C and 40 kHz. Next, the ultrasonic extract was chilled at -20 °C for 30 min, centrifuged at 4 °C for 15 min at 13,000 × g, and the supernatant was collected and dried under nitrogen. Afterward, a reconstitution solution was prepared by mixing 100 μL of acetonitrile and water in a 1:1 ratio. The dried extract was reconstituted with the reconstitution solution using an ultrasound probe for 5 min at 5 °C and 40 kHz. It was then centrifuged for 10 min at 4 °C and 13,000 × g. The supernatant was transferred to a lined injection bottle for LC-MS analysis.

UPLC-Orbitrap MS
Chromatographic separation was performed using an ACQUITY UPLC HSS T3 column (100 mm × 2.1 mm i.d., 1.8 μm; Waters, Milford, USA) preheated to 40 °C. A 2 μL serum sample was injected and analyzed at 4 °C. Samples were eluted using a mobile phase for ESI＋and ESI– consisting of 95% water and 5% acetonitrile with 0.1% formic acid as solvent A, and 47.5% acetonitrile, 47.5% isopropanol, and 5% water with 0.1% formic acid

as solvent B. The flow rate was 0.35 mL/min. The mobile phase (A: B) elution gradient was as follows: 0% for 0–1.5 min, 80%: 20% at 1.5 min, and 0%: 100% at 9.5 min, followed by 3 min of re-equilibration.

Serum metabolite analysis

Raw data were performed by ProgenesisQI (Waters Corporation, Milford, USA) for processing, and a three-dimensional data matrix in CSV format was exported. The data matrix was generated from the pre-processing results, which were composed of the retention time (RT), the mass-to-charge ratio (m/z) values, and peak intensities.

Statistical analysis

The data matrix obtained by searching the database was uploaded to the Majorbio cloud platform (https://cloud.majorbio.com) for data analysis. Fistly, data preprocessing was performed using the MetaboAnalystR package of R Studio (Version 3.3.0, https://github.com/xia-lab/MetaboAnalystR) on the Majorbio Cloud Platform. Metabolic features detected at least 80% in any set of samples were retained. To reduce the errors caused by sample preparation and instrument instability, the response intensities of the sample mass spectrometry peaks were normalized using the sum normalization method, to obtain the normalized data matrix. Meanwhile, the variables of QC samples with relative standard deviation (RSD) > 30% were excluded and log10 logarithmicized, to obtain the final data matrix for subsequent analysis.

A multivariate statistical analysis was performed using ropls package of R Studio (Version 1.6.2, http://bioconductor.org/packages/release/bioc/html/ropls.html) from Bioconductor on the Majorbio Cloud Platform. PLS-DA was used to identify metabolic variations between comparable groups. PLS-DA is a supervised learning model. To verify model reliability, group labels were randomly permuted for each sample, followed by modeling and prediction. All metabolite variables were scaled to Pareto Scaling prior to OPLS-DA analysis. Model validity was evaluated from model parameters R^2 and Q^2, which provided information about interpretability and predictability, respectively, of the model and ensured that over-fitting is avoided. Each run produced R2 and Q2 values. After 200 random permutations, regression lines for Q2 and R2 were generated. Metabolites were considered DMs if they had a P-value less than 0.05 in the Student's t-test and a Variable Importance in Projection (VIP) score above 1.0 within the PLS-DA model. Results were graphically represented in volcano plots.

For further analysis, KEGG pathway enrichment, heatmap generation, and cluster analysis were performed using Scipy in Python (version 1.0.0, https://docs.scipy.org/doc/scipy/). Additionally, the Kyoto Encyclopedia of Genes and Genomes (KEGG) database (http://www.genome.jp/kegg/, accessed on 20 October 2023) was used for metabolite pathway analysis.

Conclusion

We analyzed differences in serum metabolomics between high-altitude Tibetan and low-altitude Dezhou donkeys. Four significantly enriched metabolic pathways and nine related DMs were identified. These DMs are associated with nutrient digestion and absorption, anti-inflammatory responses, disease resistance, anti-aging, and immune function in Tibetan donkeys at high altitudes. This study provides new insights into the adaptive regulatory mechanisms of Tibetan donkeys.

Data availability

The data that support the findings of this study are openly available in the EMBL-EBI MetaboLights database (DOI: 10.1093/nar/gkad1045, PMID:37971328) reference number MTBLS10424.

References

1. Zhang, T. et al. Genome of Crucihimalaya himalaica, a close relative of Arabidopsis, shows ecological adaptation to high altitude. *Proc. Natl. Acad. Sci. U S A.* **116**, 7137–7146 (2019).
2. An, Z. et al. A homotetrameric hemoglobin expressed in alveolar epithelial cells increases blood oxygenation in high-altitude plateau pika (Ochotona curzoniae). *Cell. Rep.* **41**, 111446 (2022).
3. Guo, R. et al. Analysis of gut microbiota in chinese donkey in different regions using metagenomic sequencing. *BMC Genom.* **24**, 524 (2023).
4. Guo, R. et al. Comparison of gut microflora of donkeys in high and low altitude areas. *Front. Microbiol.* **13**, 964799 (2022).
5. Zeng, L. et al. Genomes reveal selective sweeps in kiang and donkey for high-altitude adaptation. *Zoological Res.* **42**, 450–460 (2021).
6. Zhou, Z. et al. Detection of selection signatures underlying production and adaptive traits based on whole-genome sequencing of six donkey populations. *Animals* **10**, 1823 (2020).
7. Luo, Y., Yang, X. & Gao, Y. Mitochondrial DNA response to high altitude: A new perspective on high-altitude adaptation. *Mitochondrial DNA.* **24**, 313–319 (2013).
8. B, M. & Y, L. Z, W. Genomic analysis reveals hypoxia adaptation in the Tibetan Mastiff by Introgression of the Gray Wolf from the Tibetan Plateau. *Mol. Biol. Evol.* **34**, (2017).
9. J, K. et al. The genome landscape of indigenous African cattle. *Genome Biol.* **18**, (2017).
10. Tiwari, M., Gujar, G., Shashank, C. G. & Ponsuksili, S. Selection signatures for high altitude adaptation in livestock: A review. *Gene* **927**, 148757 (2024).
11. Baranwal, G. et al. Common Metabolites in two different hypertensive mouse models: A serum and urine metabolome study. *Biomolecules* **11**, 1387 (2021).
12. Zhang, H. et al. Serum metabolomics of hyperbilirubinemia and hyperuricemia in the Tibetan plateau has unique characteristics. *Sci. Rep.* **13**, 12772 (2023).
13. Sihan, M. et al. Comparison of muscle metabolomics between two Chinese horse breeds. *Front. veterinary Sci.* **10**, (2023).

14. Zhao, J. et al. Metabolomics and transcriptomics uncover the pectin hydrolysis during tobacco stem fermentation by *Aspergillus niger*. *J. Clean. Prod.* **442**, 141005 (2024).
15. Kong, H. et al. The combination of *Brassica rapa* L. polysaccharides and cisplatin enhances the anti liver cancer effect and improves intestinal microbiota and metabolic disorders. *Int. J. Biol. Macromol.* **265**, 130706 (2024).
16. Wu, Z. et al. Construction of functional neural network tissue combining CBD-NT3-modified linear-ordered collagen scaffold and TrkC-modified iPSC-derived neural stem cells for spinal cord injury repair. *Bioactive Mater.* **35**, 242–258 (2024).
17. Jia, D. et al. Microbial metabolite enhances immunotherapy efficacy by modulating T cell stemness in pan-cancer. *Cell* **187**, 1651–1665e21 (2024).
18. Zhou, J. et al. Metabolome analysis to investigate the effect of heavy metal exposure and chemoprevention agents on toxic injury caused by a multi-heavy metal mixture in rats. *Sci. Total Environ.* **906**, 167513 (2024).
19. Kanehisa, M., Furumichi, M., Sato, Y. & Kawashima, M. Ishiguro-Watanabe, M. KEGG for taxonomy-based analysis of pathways and genomes. *Nucleic Acids Res.* **51**, D587–D592 (2023).
20. Fleishman, J. S. & Kumar, S. Bile acid metabolism and signaling in health and disease: molecular mechanisms and therapeutic targets. *Sig Transduct. Target. Ther.* **9**, 1–51 (2024).
21. Zhao, W., Wang, J., Li, X., Li, Y. & Ye, C. Deoxycholic acid inhibits *Staphylococcus aureus*-induced endometritis through regulating TGR5/PKA/NF-κB signaling pathway. *Int. Immunopharmacol.* **118**, 110004 (2023).
22. Zhao, C. et al. Gut microbiota-mediated secondary bile acid alleviates Staphylococcus aureus-induced mastitis through the TGR5-cAMP-PKA-NF-κB/NLRP3 pathways in mice. *npj Biofilms Microbiomes.* **9**, 1–15 (2023).
23. Tint, G. S., Salen, G. & Shefer, S. Effect of ursodeoxycholic acid and chenodeoxycholic acid on cholesterol and bile acid metabolism. *Gastroenterology* **91**, 1007–1018 (1986).
24. Xu, H., Zhou, S., Tang, Q., Xia, H. & Bi, F. Cholesterol metabolism: New functions and therapeutic approaches in cancer. *Biochim. Biophys. Acta Rev. Cancer*. **1874**, 188394 (2020).
25. Shastak, Y., Gordillo, A. & Pelletier, W. The relationship between vitamin A status and oxidative stress in animal production. *J. Appl. Anim. Res.* **51**, 546–553 (2023).
26. Moriyama, Y. Riboflavin transporter is finally identified. *J. Biochem.* **150**, 341–343 (2011).
27. Hustad, S. et al. Riboflavin, flavin mononucleotide, and flavin adenine dinucleotide in human plasma and erythrocytes at baseline and after low-dose riboflavin supplementation. *Clin. Chem.* **48**, 1571–1577 (2002).
28. Fischer, M. & Bacher, A. Biosynthesis of flavocoenzymes. *Nat. Prod. Rep.* **22**, 324–350 (2005).
29. Dhar-Mascareño, M., Cárcamo, J. M. & Golde, D. W. Hypoxia–reoxygenation-induced mitochondrial damage and apoptosis in human endothelial cells are inhibited by vitamin C. *Free Radic. Biol. Med.* **38**, 1311–1322 (2005).
30. Purkayastha, S. S. et al. Effect of vitamin C and E in modulating peripheral vascular response to local cold stimulus in man at high altitude. *Jpn J. Physiol.* **49**, 159–167 (1999).
31. Wei, X. S. et al. Effects of biotin and nicotinamide supplementation on glucose and lipid metabolism and milk production of transition dairy cows. *Anim. Feed Sci. Technol.* **237**, 106–117 (2018).
32. Seo, S. K. & Kwon, B. Immune regulation through tryptophan metabolism. *Exp. Mol. Med.* **55**, 1371–1379 (2023).
33. Gao, J. et al. Metabolomic analysis of human plasma sample after exposed to high altitude and return to sea level. *PLOS ONE.* **18**, e0282301 (2023).
34. Basran, J. et al. The mechanism of formation of N-formylkynurenine by heme dioxygenases. *J. Am. Chem. Soc.* **133**, 16251–16257 (2011).
35. De la Muñoz, F. Effects of supplementation with the standardized extract of Saffron (affron*) on the Kynurenine pathway and melatonin synthesis in rats. *Antioxidants***12**, 1619 (2023).
36. Attanasio, A., Rager, K. & Gupta, D. Ontogeny of circadian rhythmicity for melatonin, serotonin, and N-acetylserotonin in humans. *J. Pineal Res.* **3**, 251–256 (1986).
37. Muneer, A. Kynurenine pathway of tryptophan metabolism in neuropsychiatric disorders: Pathophysiologic and therapeutic considerations. *Clin. Psychopharmacol. Neurosci.* **18**, 507 (2020).
38. Davidson, M., Rashidi, N., Nurgali, K. & Apostolopoulos, V. The role of tryptophan metabolites in neuropsychiatric disorders. *Int. J. Mol. Sci.* **23**, (2022).
39. Song, T. T. et al. Systemic pro-inflammatory response facilitates the development of cerebral edema during short hypoxia. *J. Neuroinflammation.* **13**, 1–14 (2016).
40. Bruschetta, G., Fazio, E., Cravana, C. & Ferlazzo, A. M. Effects of partial versus complete separation after weaning on plasma serotonin, tryptophan and pituitary-adrenal pattern of Anglo-Arabian foals. *Livest. Sci.* **198**, 157–161 (2017).
41. Watson, P. H. & Hanley, D. A. Parathyroid hormone: regulation of synthesis and secretion. *Clin. Invest. Med.* **16**, 58–77 (1993).
42. Ursem, S. R., Vervloet, M. G., de Jongh, R. T. & Heijboer, A. C. Oxidation of parathyroid hormone. *Clin. Chim. Acta*. **506**, 84–91 (2020).
43. Yasuda, K. et al. UV-dependent production of 25-hydroxyvitamin D2 in the recombinant yeast cells expressing human CYP2R1. *Biochem. Biophys. Res. Commun.* **434**, 311–315 (2013).
44. Lisakovska, O., Shymanskyi, I., Labudzynskyi, D., Mazanova, A. & Veliky, M. Vitamin D Auto-/paracrine system is involved in modulation of glucocorticoid-induced changes in angiogenesis/bone remodeling coupling. *Int. J. Endocrinol.* **8237610** (2020). (2020).
45. Wu, P. et al. Liver Injury Impaired 25-Hydroxylation of Vitamin D Suppresses Intestinal Paneth Cell defensins, leading to Gut Dysbiosis and Liver Fibrogenesis. *Am. J. Physiol. Gastrointest. Liver Physiol.* **319**, G685–695 (2020).
46. Warnke, M. et al. 25-Hydroxyvitamin D3 Synthesis by Enzymatic Steroid Side-Chain Hydroxylation with Water. *Angew Chem. Int. Ed. Engl.* **55**, 1881–1884 (2016).
47. Alnasser, H. A. et al. Requirement of clusterin expression for prosurvival autophagy in hypoxic kidney tubular epithelial cells. *Am. J. Physiol. Ren. Physiol.* **310**, F160–173 (2016).
48. Sun, B., Maruta, H., Ma, Y. & Yamashita, H. Taurine Stimulates AMP-Activated Protein Kinase and Modulates the Skeletal Muscle Functions in Rats via the Induction of Intracellular Calcium Influx. *Int. J. Mol. Sci.* **24**, 4125 (2023).
49. Sharma, A., Anand, S. K., Singh, N., Dwivedi, U. N. & Kakkar, P. AMP-activated protein kinase: An energy sensor and survival mechanism in the reinstatement of metabolic homeostasis. *Exp. Cell. Res.* **428**, 113614 (2023).
50. Fryer, L. G. D., Parbu-Patel, A. & Carling, D. The Anti-diabetic drugs rosiglitazone and metformin stimulate AMP-activated protein kinase through distinct signaling pathways. *J. Biol. Chem.* **277**, 25226–25232 (2002).

Acknowledgements

Author contributions

S.L. and Y.S. planned and designed the experiments and contributed to writing the manuscript. J.W. and Y.F. conducted the experiments, analyzed the data, and wrote the original manuscript. S.X, N.T.,H.H., F.L., and D.G. collected the samples. All authors reviewed the manuscript.

Competing interests
The authors declare no competing interests.

Ethics approval and consent to participate
This study was approved by the Animal Care and Use Committee of Qingdao Agricultural University (Qingdao, Shandong Province, China). This study was reported in accordance with ARRIVE guidelines.

Consent for publication
Not Applicable.

Additional information
Supplementary Information The online version contains supplementary material available at https://doi.org/10.1038/s41598-024-83544-8.

Correspondence and requests for materials should be addressed to Y.S. or S.L.

Reprints and permissions information is available at www.nature.com/reprints.

Publisher's note Springer Nature remains neutral with regard to jurisdictional claims in published maps and institutional affiliations.